Ditungsten Siloxide Hydrides, $[(silox)_2WH_n]_2$ (n = 1, 2; silox = ^{t}BuSiO), and Related Complexes

Rebecca L. Miller, Kimberly A. Lawler, Jordan L. Bennett, and Peter T. Wolczanski*

Baker Laboratory, Department of Chemistry, Cornell University, Ithaca, New York 14853

Received October 16, 1995[⊗]

The addition of 4.0 equiv of Na(silox) to $Na[W_2Cl_7(THF)_5]$ afforded $(silox)_2ClW{\equiv}WCl(silox)_2$ (**1**, 65%). Treatment of **1** with 2.0 equiv of MeMgBr in Et_2O provided $(silox)_2MeW{\equiv}WMe(silox)_2$ (**2**, 81%). In the presence of 1 atm of H_2, reduction of **1** with 2.0 equiv of Na/Hg in DME provided $(silox)_2HW{\equiv}WH(silox)_2$ (**3**, 70%), characterized by a hydride resonance at δ 19.69 (J_{WH} = 325 Hz, ^{1}H NMR). Exposure of **2** to 1 atm of H_2 yielded **3** and CH_4 via $(silox)_2HW{\equiv}WMe(silox)_2$ (**4**); use of D_2 led to $[(silox)_2WD]_2$ (**3**-d_2). Exposure of **3** to ethylene (∼1 atm, 25 °C) in hexanes generated $(silox)_2EtW{\equiv}WEt(silox)_2$ (**5**), but solutions of **5** reverted to **3** and free C_2H_4 upon standing. NMR spectral data are consistent with a sterically locked, *gauche*, C_2 symmetry for **1**−**5**. Thermolysis of **3** at 100 °C (4 h) resulted in partial conversion to $(silox)_2HW{\equiv}W(OSi^tBu_2CMe_2CH_2)(silox)$ (**6a**, ∼60%) and free H_2, while extended thermolysis with degassing (5 d, 70 °C) produced a second cyclometalated rotational isomer, **6b** (**6a**:**6b** ∼ 3:1). When left at 25 °C (4 h) in sealed NMR tubes, **6** and free H_2 regenerated **3**. Reduction of **1** with 2.0 equiv of Na/Hg in DME also afforded **6a** (25%). When **3** was exposed to ∼3 atm of H_2, equilibrium amounts of $[(silox)_2WH_2]_2$ (**7**) were observed by ^{1}H NMR spectroscopy (**3** + H_2 ⇌ **7**; 25.9−88.7 °C, ΔH = −9.6(4) kcal/mol, ΔS = −21(2) eu). Benzene solutions of **3** and 1−3 atm of D_2 revealed incorporation of deuterium into the silox ligands, presumably via intermediate **6**. In sealed tubes containing $[(silox)_2WCl]_2$ (**1**) and dihydrogen (1−3 atm), ^{1}H NMR spectral evidence for $[(silox)_2WCl]_2(\mu$-H$)_2$ (**8**) was obtained, suggesting that formation of **3** from **1** proceeded via reduction of **8**. Alternatively, **3** may be formed from direct reduction of **1** to give $[(silox)_2W]_2$ (**9**), followed by H_2 addition. Hydride chemical shifts for **7** are temperature dependent, varying from δ 1.39 (−70 °C, toluene-d_8), to δ 3.68 (90 °C). ^{29}Si{^{1}H} NMR spectra revealed a similar temperature dependence of the silox (δ 12.43, −60 °C, to δ 13.64, 45 °C) resonances. These effects may arise from thermal population of a low-lying, $\delta\delta^*$, paramagnetic excited state of D_{2d} $[(silox)_2W]_2(\mu$-H$)_4$ (ΔE ∼ 2.1 kcal/mol, χ(**7a***) ∼ 0.03), an explanation favored over thermal equilibration with an energetically similar but structurally distinct isomer (e.g., $[(silox)_2WH_2]_2(\mu$-H$)_2$, $\Delta G°$ ∼ 0.69 kcal/mol, χ(**7b**) ∼ 0.25) on the basis of spectral arguments. Extended Hückel and *ab initio* molecular orbital calculations on model complexes $[(H_3SiO)_2W]_2(\mu$-H$)_4$ (staggered bridged **7a′**, EHMO), $[(H_3SiO)_2WH_2]_2$ (all-terminal **7b′**, EHMO), $[(H_3SiO)_2W]_2$ (**9′**, EHMO), $(HO)_4W_2(H_4)$ (staggered-bridged **7″**, *ab initio*), and $(HO)_4W_2(H_4)$ (bent-terminal **7***, *ab initio*) generally support the explanation of a thermally accessible excited state and assign **7*** a geometry intermediate between the all-terminal and staggered-bridged forms.

Introduction

Transition metal hydride complexes have generated intense study, both as reactive species in homogeneous stoichiometric and catalytic transformations and as models for metal−hydrogen interactions in heterogeneous systems.[1] Discrete, well-characterized hydride and polyhydride complexes have become common since discovery of the classic carbonyl hydrides.[2] The vast majority contain ancillary cyclopentadienyl, related π-hydrocarbon, and phosphine ligands that tend to electronically and sterically saturate a metal center, rendering it "soft". As a consequence, hydride complexes in low to middle oxidation states abound, and equilibria with related dihydrogen species are sometimes apparent.[3]

In contrast, transition metal compounds containing hydrides supported exclusively by hard, π-donor ligands such as alkoxides, siloxides, and amides are limited.[4] Almost exclusively early transition metal species, these hydrides often possess fundamentally different properties and reactivity patterns relative to lower valent congeners. Carbonylation of $[(silox)_2TaH_2]_2$ (silox = ^{t}Bu$_3$SiO$^-$) leads to CO bond-breaking and C−H and C−C bond-making events *en route* to $[(silox)_2Ta]_2(\mu$-O$)_2(\mu$-CHMe$)(\mu$-O$)_2$,[5] while related phosphine-[6] and cyclopentadienyl-based systems[7−9] exhibit no carbon monoxide reduction. The catalytic potential of alkoxide hydrides is exemplified by the all-*cis* hydrogenation of polynuclear aromatics by hydrides

⊗ Abstract published in *Advance ACS Abstracts,* April 15, 1996.

(1) (a) Collman, J. P.; Hegedus, L. S.; Norton, J. R.; Finke, R. G. *Principles and Applications of Organotransition Metal Chemistry*; University Science Books: Mill Valley, CA, 1987. (b) Parshall, G. W.; Ittel, S. D. *Homogeneous Catalysis*; Wiley-Interscience: New York, 1992. (c) Gates, B. C. *Catalytic Chemistry*; John Wiley & Sons: New York, 1992.

(2) (a) Moore, D. S.; Robinson, S. D. *Chem. Soc. Rev.* **1983**, *12*, 415−452. (b) Hlatky, G. G.; Crabtree, R. H. *Coord. Chem. Rev.* **1985**, *65*, 1−48.

(3) (a) Kubas, G. J. *Acc. Chem. Res.* **1988**, *21*, 120−128. (b) Jessop, P. G.; Morris, R. H. *Coord. Chem. Rev.* **1992**, *121*, 155−284. (c) Heinekey, D. M.; Oldham, W. J. *Chem. Rev.* **1993**, *93*, 913−926. (d) Crabtree, R. H. *Acc. Chem. Res.* **1990**, *23*, 95−101.

(4) Chisholm, M. H. *Chem. Soc. Rev.* **1995**, *24*, 79−87.

(5) Miller, R. L.; Toreki, R.; LaPoint, R. E.; Wolczanski, P. T.; Van Duyne, G. D.; Roe, D. C. *J. Am. Chem. Soc.* **1993**, *115*, 5570−5588.

(6) Scioly, A. J.; Luetkens, M. L.; Wilson, R. B., Jr.; Huffman, J. C.; Sattelberger, A. P. *Polyhedron* **1987**, *6*, 741−757 and references therein.

(7) (a) Tebbe, F. N.; Parshall, G. W. *J. Am. Chem. Soc.* **1971**, *93*, 3793−3795. (b) Tebbe, F. N. *J. Am. Chem. Soc.* **1973**, *95*, 5412−5414. (c) Barefield, E. K.; Parshall, G. W.; Tebbe, F. N. *J. Am. Chem. Soc.* **1970**, *92*, 5234−5235. (d) Green, M. L. H.; McCleverty, J. A.; Pratt, L.; Wilkinson, G. *J. Chem. Soc.* **1961**, 4854−4859.

(8) Gibson, V. C.; Bercaw, J. E.; Bruton, W. J.; Sanner, R. D. *Organometallics* **1986**, *5*, 976−979.

S0020-1669(95)01319-X CCC: $12.00

generated via H_2-mediated cleavage of the metal−benzyl bonds in $Nb(OC_6H_3\text{-}2,6\text{-}Ph_2)_2(CH_2C_6H_4\text{-}4\text{-}Me)_3$;[10] convenient syntheses of cyclohexyl- and methylenecyclohexylphosphine species derived from aromatic precursors have also been reported.[11]

Hydrides containing hard, ancillary π-donor ligands have not been synthesized through the addition of H^- equivalents, and only rarely through mononuclear oxidative addition,[12] because low-valent precursors are uncommon. Hydrogenation of metal−alkyl bonds represents a sound route,[9] but subsequent aggregation of the hydride(s) must often be prevented through addition of other ligands, typically phosphines (e.g., $(2,6\text{-}Cy_2H_3C_6O)_3TaH_2(PMe_2Ph)$, $(2,6\text{-}Cy_2H_3C_6O)_2TaH_3(PMe_2Ph)_2$).[13,14] Because of the high pressures usually required, mechanistic studies of these hydrogenations have been limited, although σ-bond metathesis appears to be the most likely process.[15] A recent preparation of an intriguing thorium alkoxide hydride, $Th_3(\mu_3\text{-}H)_2(\mu\text{-}H)_4(O\text{-}2,6\text{-}{}^tBu_2C_6H_3)_6$, utilized hydrogenation of a precursor dialkyl, but the pathway is unknown.[16]

Some interesting alkoxide hydrides have been generated via unexpected pathways. $Re_3(O^iPr)_9$ undergoes β-elimination to form $Re_3(O^iPr)_8H$ and acetone, a reaction typical of low-valent, late transition metal complexes.[17] While the reaction is reversible and approximately thermoneutral for the sterically encumbered Re(III) cluster, corresponding β-eliminations are expected to be thermodynamically disfavored for high-valent early metals whose bonds to oxygen are much stronger. A related degradation of a *tert*-butoxide ligand in $[W_2(O^tBu)_7]^-$ yielded $\{[(^tBuO)_3W]_2(\mu\text{-}O)(\mu\text{-}H)\}^-$ through γ-C−H activation, and concomitant isobutylene elimination incurred via a six-membered transition state.[18]

Several tungsten alkoxy hydrides have been discovered in alcoholyses of ditungsten hexaamides, $W_2(NR_2)_6$.[19] The first such example, $[W_2(\mu\text{-}H)(O^iPr)_7]_2$, was prepared by reaction of excess 2-propanol with $W_2(NMe_2)_6$.[20] Conceptually, the hydride complex is derived from alcoholysis of the amides, followed by oxidative addition of $^iPrO-H$ across across the W≡W bond and subsequent dimerization. $NaW_2(\mu\text{-}H)(O^iPr)_8$, $NaW_2(\mu\text{-}H)(OCH_2{}^tBu)_8$, $W_2I(\mu\text{-}H)(OCH_2{}^tBu)_6(H_2NMe)$, and $W_2(\mu\text{-}H)(O\text{-}c\text{-}C_5H_9)_7(HNMe_2)$ were prepared by related procedures.

Oxidative addition of dihydrogen across the metal−metal bonds of appropriate precursors is an appealing route to new hydrides, but aggregation phenomena again render this method unpredictable. Hydrogenolysis of $W_2(^iBu)_2(O^iPr)_4$ is initiated by addition of H_2 across the W≡W bond, causing elimination of isobutane and $H_2C{=}CMe_2$. The resulting binuclear transients cluster to form an intriguing hexanuclear derivative, $W_6(\mu\text{-}H)_4(\mu\text{-}O^iPr)_7(\mu\text{-}C^iPr)(H)(O^iPr)_5$ or become trapped in the presence of dmpe to provide $W_2H_2(O^iPr)_6(dmpe)_2$.[21] A related tetranuclear $Mo^{II}{}_2/Mo^{III}{}_2$ butterfly species, $(^tBuO)_7H_3Mo_4(HNMe_2)$, was formed upon hydrogenation of $1,2\text{-}(Me_2N)_4(p\text{-tolyl})_2Mo_2$ in the presence of ^tBuOH.[22]

The aggregation and clusterification phenomena evidenced by early transition metal alkoxide hydrides have three principal origins. First, high oxidation state $(RO)_nMH_m$ complexes possess an inherent electronic unsaturation conducive to the binding of additional donors. Second, multicenter interactions are common for highly polar bonds, such as early transition metal alkoxides and hydrides. While $O(p\pi) \rightarrow M(d\pi)$ bonding is strong, formation of a second or even a third σ-bond effectively competes with π-donation. Finally, steric compensation for the extremely small hydride ligand must be provided by the ancillary alkoxides in order to prevent aggregation of the electrophilic metal centers. Few alkoxides/siloxides meet such stringent steric demands.[4]

Aggregate formation has been circumvented through use of the extremely bulky silox ($^tBu_3SiO^-$) ligand,[23,24] leading to titanium,[25] tantalum, and niobium hydrides of predictable nuclearity. Oxidative addition of H_2 to $(silox)_3Ta$ afforded $(silox)_3TaH_2$,[12] while structural models suggest that bis(silox) ligation favors dimeric species. Accordingly,[21] treatment of $(silox)_2MCl_3$ with excess Na/Hg under 1 atm of dihydrogen for long durations yielded thermally robust $[(silox)_2MH_2]_2$ (M = Nb, Ta) in moderate to excellent yields.[5,26] In addition, the silox ligand has been remarkably resilient when ligating lower valent metal centers, such as Ti(III),[27] V(III), Ta(III),[28] Nb(IV), and Ta(IV) in $[(silox)_2MH_2]_2$ and W(III) in W≡W derivatives.[29]

With these precedents, routes to tetrakis(silox)ditungsten hydrides were explored. Described herein are various discrete, dinuclear hydrides of tungsten generated through addition of H_2 to W≡W fragments. Extended Hückel molecular orbital (EHMO) and *ab initio* calculations explore the validity of the structural assignment of $[(silox)_2WH_2]_2$ and are used to generate a rough electronic structure of quadruply bonded $[(silox)_2W]_2$, a plausible reaction intermediate.

Results

Synthesis and Characterization of $(silox)_2XW{\equiv}WX(silox)_2$ (X: Cl, 1; Me, 2; H, 3; Et, 5). A convenient preparation of $(silox)_2ClW{\equiv}WCl(silox)_2$ (**1**) utilized the versatile ditungsten-

(9) Mayer, J. M.; Wolczanski, P. T.; Santarsiero, B. D.; Olson, W. A.; Bercaw, J. E. *Inorg. Chem.* **1983**, *22*, 1149−1154 and references therein.
(10) Yu, J. S.; Ankianiec, B. C.; Nguyen, M. T.; Rothwell, I. P. *J. Am. Chem. Soc.* **1992**, *114*, 1927−1929.
(11) Yu, J. S.; Rothwell, I. P. *J. Chem. Soc., Chem. Commun.* **1992**, 632−633.
(12) For a pertinent example, see: Neithamer, D. R.; LaPointe, R. E.; Wheeler, R. A.; Richeson, D. S.; Van Duyne, G. D.; Wolczanski, P. T. *J. Am. Chem. Soc.* **1989**, *111*, 9056−9072.
(13) (a) Visciglio, V. M.; Fanwick, P. E.; Rothwell, I. P. *J. Chem. Soc., Chem. Commun.* **1992**, 1505−1507. (b) Ankianiec, B. C.; Fanwick, P. E.; Rothwell, I. P. *J. Am. Chem. Soc.* **1991**, *113*, 4710−4712.
(14) Parkin, B. C.; Clark, J. R.; Visciglio, V. M.; Fanwick, P. E.; Rothwell, I. P. *Organometallics* **1995**, *14*, 3002−3013.
(15) Thompson, M. E.; Baxter, S. M.; Bulls, A. R.; Burger, B. J.; Nolan, M. C.; Santarsiero, B. D.; Schaefer, W. P.; Bercaw, J. E. *J. Am. Chem. Soc.* **1987**, *109*, 203−219.
(16) Clark, D. L.; Grumbine, S. K.; Scott, B. L.; Watkin, J. G. *J. Am. Chem. Soc.* **1995**, *117*, 9089−9090.
(17) Hoffman, D. M.; Lappas, D.; Wierda, D. A. *J. Am. Chem. Soc.* **1993**, *115*, 10538−10544.
(18) Budzichowski, T. A.; Chisholm, M. H.; Strieb, W. E. *J. Am. Chem. Soc.* **1994**, *116*, 389−390.
(19) Akiyama, M.; Chisholm, M. H.; Cotton, F. A.; Extine, M. W.; Haitko, D. A.; Leonelli, J.; Little, D. *J. Am. Chem. Soc.* **1981**, *103*, 779−784.
(20) (a) Chisholm, M. H.; Huffman, J. C.; Smith, C. A. *J. Am. Chem. Soc.* **1986**, *108*, 222−230. (b) Chacon, S. T.; Chisholm, M. H.; Folting, K.; Hampden-Smith, M. J.; Huffman, J. C. *Inorg. Chem.* **1991**, *30*, 3122−3125.
(21) Chisholm, M. H.; Kramer, K. S.; Streib, W. E. *J. Am. Chem. Soc.* **1992**, *114*, 3571−3573. Correction: *J. Am. Chem. Soc.* **1995**, *114*, 6152.
(22) Chisholm, M. H.; Huffman, J. C.; Kramer, K. S.; Streib, W. E. *J. Am. Chem. Soc.* **1993**, *115*, 9866−9867.
(23) (a) Weidenbruch, M.; Pierrard, C.; Pesel, H. Z. *Naturforsch., B: Anorg. Chem. Org. Chem.* **1978**, *33B*, 1468−1471. (b) Dexheimer, E. M.; Spialter, L.; Smithson, L. D. *J. Organomet. Chem.* **1975**, *102*, 21−27.
(24) LaPointe, R. E.; Wolczanski, P. T.; Van Duyne, G. D. *Organometallics* **1985**, *4*, 1810−1818.
(25) Bennett, J. L.; Wolczanski, P. T. *J. Am. Chem. Soc.* **1994**, *116*, 2179−2180.
(26) LaPointe, R. E.; Wolczanski, P. T. *J. Am. Chem. Soc.* **1986**, *108*, 3535−3537.
(27) Covert, K. J.; Wolczanski, P. T.; Hill, S. A.; Krusic, P. J. *Inorg. Chem.* **1992**, *31*, 66−78.
(28) Covert, K. J.; Neithamer, D. R.; Zonnevylle, M. C.; LaPointe, R. E.; Schaller, C. P.; Wolczanski, P. T. *Inorg. Chem.* **1991**, *30*, 2494−2508.
(29) Miller, R. L.; Wolczanski, P. T.; Rheingold, A. L. *J. Am. Chem. Soc.* **1993**, *115*, 10422−10423.

Scheme 1

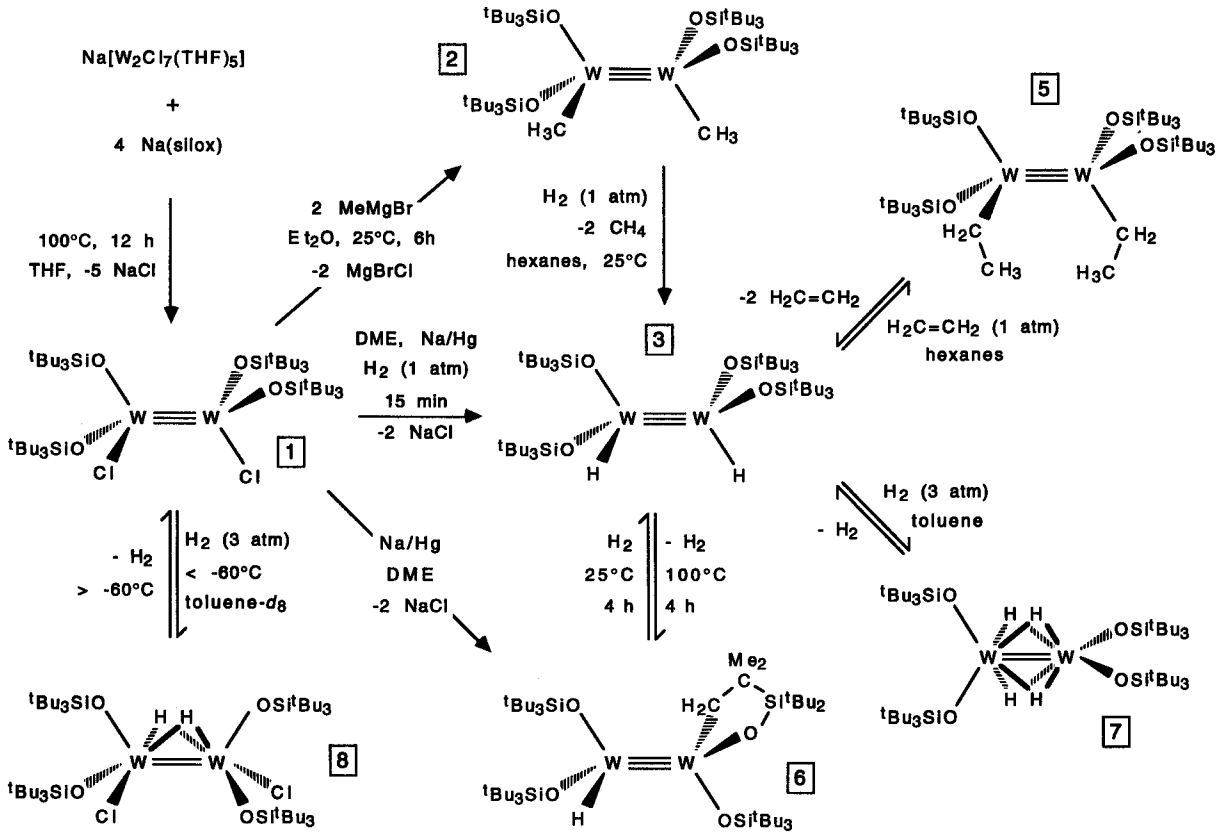

(III) precursor $Na[W_2Cl_7(THF)_5]$,[30] which was generated by Na/Hg reduction of WCl_4 in THF,[31] and transferred directly into a reaction vessel containing 4.0 equiv of Na(silox) (Scheme 1).[29] After refluxing of the solution for 12 h, followed by workup in hexanes, **1** was isolated as brown crystals in 65% overall yield, based on WCl_4. Comparable yields were achieved when crystalline $Na[W_2Cl_7(THF)_5]$ was used as the precursor.

Inequivalent silox ligands evidenced in ^1H and $^{13}C\{^1H\}$ NMR spectra (Table 1) of **1** reflect a *gauche*, C_2 symmetry, assuming the staggered geometry common to $X_2YM{\equiv}MX_2Y$ (M = Mo, W) species.[32,33] In previous cases, the preference for a *gauche* conformer was rationalized through consideration of steric interactions across the M≡M bond, and the alternative *anti* structure was often observed in solution. No indication of the *anti* configuration was present in the NMR spectra of **1** and variable-temperature ^1H NMR studies (25−120 °C) failed to reveal coalescence ($\Delta G^{\ddagger} > 21$ kcal/mol). Figure 1 illustrates Newman projections for both *anti* and *gauche* conformations. According to previous rationale, the *gauche* species is more stable if the combination of (silox)|(silox) and Cl|Cl interactions are less sterically demanding than two (silox)|Cl interactions of the *anti* form.

The tremendous bulk of the $^tBu_3SiO$ group, previously shown to exert substantial influence on both structure and chemical reactivity,[5,12,27−29] may cause a distortion within each $(silox)_2$ClW fragment that obviates conventional steric interpretations. As shown, a distortion of the tungsten coordination toward the trigonal pyramidal geometry allows the $(silox)_4W_2$ fragment to approach a D_{2d} arrangement,[5] driving the chlorides into a pseudoeclipsing orientation. A bis-bridging chloride structure appears to be sterically precluded because two silox groups abut parallel to the metal−metal bond; no precedent for such $X_2YM{\equiv}MX_2Y$ (M = Mo, W) structures exists. In corroboration, related $(silox)_2XW{\equiv}WX(silox)_2$ (X = H, Me, Et) complexes all manifest the same C_2 symmetry (*vide infra*), and none exhibit measurable dynamic behavior. X-ray crystallographic characterizations of these complexes have been continually hampered by poor-quality crystals; efforts are continuing.

Treatment of dichloride **1** with 2.0 equiv of MeMgBr in Et_2O afforded the green dimethyl complex $(silox)_2(H_3C)W{\equiv}W(CH_3)(silox)_2$ (**2**) in 81% yield upon crystallization from hexanes. Inequivalent silox and equivalent methyl resonances in the ^1H and $^{13}C\{^1H\}$ NMR spectra indicate a C_2 structure analogous to the dichloride (**1**). The methyl protons (δ 3.70, J_{CH} = 124 Hz) exhibit a small, 2-bond coupling of J_{WH} = 12 Hz to tungsten, while the methyl carbon (δ 44.43) manifests a normal 1-bond J_{WC} of 124 Hz.[34]

In the presence of 1 atm of H_2, reduction of dichloride **1** with 2.0 equiv of Na/Hg in DME provided $(silox)_2HW{\equiv}WH(silox)_2$ (**3**), which was isolated as brown crystals from hexane in somewhat sporadic yields approaching 70%. Dihydride **3** degraded slowly under the reaction conditions to form Na(silox)

(30) Chisholm, M. H.; Eichorn, B. W.; Folting, K.; Huffman, J. C.; Ontiveros, C. D.; Streib, W. E.; Van Der Sluys, W. G. *Inorg. Chem.* **1987**, *26*, 3182−3186.
(31) Schrock, R. R.; Sturgeoff, L. G. Sharp, P. R. *Inorg. Chem.* **1983**, *22*, 2801−2806.
(32) Cotton, F. A.; Walton, R. A. *Multiple Bonds Between Metal Atoms*, 2nd ed.; Oxford University Press: New York, 1993; see also references therein.
(33) (a) Chisholm, M. H.; Rothwell, I. P. *Prog. Inorg. Chem.* **1982**, *29*, 1−72. (b) Chisholm, M. H.; Hoffman, D. M.; Huffman, J. C. *Chem. Soc. Rev.* **1985**, *14*, 69−91. (c) Green, M. L. H.; Mountford, P. P. *Chem. Soc. Rev.* **1992**, *21*, 29−39.
(34) (a) Chisholm, M. H.; Cotton, F. A.; Extine, M.; Millar, M.; Stults, B. R. *J. Am. Chem. Soc.* **1976**, *98*, 4486−4491. (b) Akiyama, M.; Chisholm, M. H.; Cotton, F. A.; Extine, M. W.; Murillo, C. A. *Inorg. Chem.* **1977**, *16*, 2407−2411. (c) Chisholm, M. H.; Cotton, F. A.; Extine, M.; Millar, M.; Stults, B. R. *Inorg. Chem.* **1977**, *16*, 320−328. (d) Chisholm, M. H.; Huffman, J. C.; Pasterczyk, J. W. *Inorg. Chem.* **1987**, *26*, 3781−3785. (e) Chisholm, M. H.; Hampden-Smith, M. J.; Huffman, J. C.; Moodley, K.G. *J. Am. Chem. Soc.* **1988**, *110*, 4070−4071.

Table 1. NMR [δ in ppm (Multiplicity, J in Hz, Assignment)][a] and IR (cm^{-1})[b] Data for Dinuclear Tungsten Chloride, Hydride, and Alkyl Complexes

	^1H[c]			^{13}C or $^{13}C\{^1H\}$[d]		
compound	silox	WH	other	$Si(C(CH_3)_3)_3$[e]	other	IR ν(WH)
$[(silox)_2ClW]_2$ (**1**)	1.25			24.16, 24.53		
	1.28			30.89, 31.00		
$[(silox)_2MeW]_2$ (**2**)	1.20		3.70 (s, Me)	23.76, 24.08	44.43 (Me)	
	1.28		$J_{WH} = 12$	30.91, 31.01	$J_{WC} = 124$	
$[(silox)_2HW]_2$ (**3**)	1.22	19.69		23.13, 23.18		1995[f]
	1.30	$J_{WH} = 325$		30.47, 30.50		
$[(silox)_2(CH_3CH_2)W]_2$ (**5**)	1.24		2.20 (t, 7.5, Me)	23.58, 23.77	19.12 (Me)	
	1.29		3.87 (dq, 15, 7, CH*H*)	31.10, 31.46	59.93 (CH_2)	
			5.42 (dq, 15, 7, C*H*H)		$J_{WC} = 120$	
					$J_{CC} = 32$[g]	
$(silox)_2HW\overline{W(OSi^tBu_2CMe_2CH_2)}(silox)$						
(**6a**)	1.15	18.67	1.23, 1.33 ($^tBu_2$)	22.86, 23.71, 22.86	22.35, 23.29 (SiC)	1995[f]
	1.24	$J_{WH} = 336$	1.50, 1.52 (Me_2)	30.41, 30.82, 30.86	23.20 (CMe_2)	
	1.32		3.66 (d, 13, CH*H*)		29.10 (WCH_2)	
			3.90 (d, 13, C*H*H)		29.46, 30.22 ($C(CH_3)_3)_2$	
					34.18, 34.29 ($C(CH_3)_2$)	
(**6b**)	1.07	18.29	($^tBu_2$)[h]			
	1.29	$J_{WH} = 313$	1.88, 1.91 (Me_2)			
	1.43		(CH_2)[h]			
$[(silox)_2W]_2(\mu\text{-}H)_4$ (**7**, 25 °C[i], C_7D_8)	1.29	2.67				
		$J_{W2H} = 104$				
$[(silox)_2ClW]_2(\mu\text{-}H)_2$ (**8**, −84 °C, C_7D_8)	1.31 (br)	15.12				
		$J_{W2H} = 115$				

[a] Benzene-d_6 unless otherwise noted. J_{WH} indicates an integrated satellite intensity ~14%. J_{W2H} indicates an integrated satellite intensity ~25%. [b] Nujol. [c] Referenced to Me_4Si at δ 0.0 or benzene-d_6 at δ 7.15. [d] Referenced to benzene-d_6 at δ 128.00. [e] Assignments: δ ~24, CH_3; δ ~31, CMe_3. [f] Broad ν(WH). [g] Obtained from $(silox)_2(^{13}CH_3{}^{13}CH_2)W]_2$ (**5**-($^{13}CH_2{}^{13}CH_3)_2$). [h] Presumably obscured. [i] ^1H (hydride, δ 1.39 (−70 °C), δ 3.68 (90 °C) and $^{29}Si\{^1H\}$ (silox, δ 12.43 (−60 °C), δ 13.64 (45 °C)) shifts are temperature dependent.

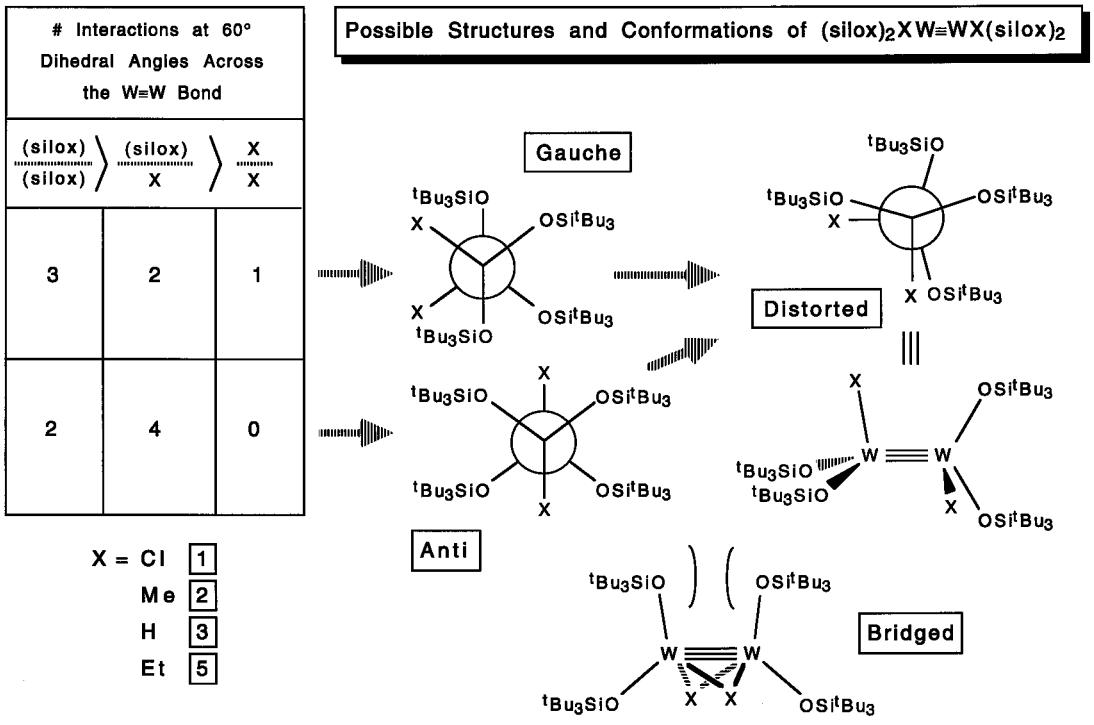

Figure 1.

and other byproducts, possibly via attack of chloride ion at the electrophilic tungsten centers. Similar reductions using Mg^0 powder were slower and gave colorless $Mg(silox)_2$ as the only isolable material. Dihydride **3** again displays C_2 molecular symmetry through the inequivalence of its silox ligands in ^1H and $^{13}C\{^1H\}$ NMR spectra. A single hydride resonance appears at δ 19.69 in the ^1H spectrum, with $J_{WH} = 325$ Hz (~14% integrated intensity), a large coupling consistent with a terminal binding mode. A moderately strong ν(WH) of 1995 cm^{-1} in the infrared spectrum corroborated this assignment.

Exposure of $[(silox)_2WMe]_2$ (**2**) to dihydrogen (1 atm) also yielded dihydride **3** and concomitant methane, and when D_2 was used, $[(silox)_2WD]_2$ (**3**-d_2) was conveniently prepared. A distinct ν(WD) is absent in its IR spectrum, but this absorption is predicted to lie directly under a melange of strong silox C−H bands (ca. 1450 cm^{-1}). Only CH_3D was produced upon deuteration, supporting a mechanism predicated on initial oxidative addition of D_2 across the W≡W bond. In monitoring the hydrogenation of **2** by ^1H NMR, singlet hydride (δ 19.51, $J_{WH} = 335$ Hz) and methyl (δ 3.96, $J_{WH} = 11.4$ Hz) resonances

were observed to appear (~20%) and then fade as the conversion to **3** (and equilibrium amounts of $[(silox)_2W]_2(\mu\text{-}H)_4$ (**7**)) was completed. The signals are tentatively assigned to an intermediate methyl−hydride complex, $(silox)_2HW{\equiv}WMe(silox)_2$ (**4**), thereby supporting the postulated mechanism.

Exposure of $[(silox)_2WH]_2$ (**3**) to excess ethylene (~1 atm) in hexanes rapidly generated brown-black $(silox)_2(CH_3CH_2)W{\equiv}W(CH_2CH_3)(silox)_2$ (**5**) at 25 °C. Due to the C_2 molecular symmetry, the methylene protons of **5** are diastereotopic in the ^{1}H NMR spectrum, resonating at δ 3.87 and 5.42 ($J_{HH'} = 15$ Hz). The corresponding methylene ^{13}C NMR resonance at δ 59.93 exhibits a normal sp^3 J_{CH} of 125 Hz, a typical 1-bond J_{WC} of 120 Hz,[32] and a J_{CC} of 32 Hz indicative of an sp^3−sp^3 carbon−carbon bond.[35] The latter was observed upon synthesis of **5**-($^{13}CH_2{}^{13}CH_3)_2$ from **3** and $^{13}C_2H_4$. Ethylene insertion/deinsertion is approximately thermoneutral, since solutions of **5** reverted to dihydride **3** and free C_2H_4 upon standing for a few hours.

Cyclometalations. Thermolysis of $[(silox)_2WH]_2$ (**3**) at 100 °C for 4 h resulted in partial conversion to a cyclometalated product, $(silox)_2HW{\equiv}W(OSi^tBu_2CMe_2CH_2)(silox)$ (**6a**, ~60%), and free H_2. The cyclometalated silox group displays inequivalent *tert*-butyl and methyl groups in the ^{1}H NMR spectrum and diastereotopic methylene protons (δ 3.66, 3.90, $J_{HH'} = 13$ Hz). A terminal hydride appears at δ 18.67 ($J_{HW} = 336$ Hz), with a corresponding IR absorption at 1995 cm^{-1}. Extended thermolysis of **3** with requisite degassing (5 d, 70 °C) in cyclohexane revealed two rotational isomers, **6a** and **6b**, in a ~3:1 ratio. Upon further heating of the mixture in C_6D_6 (15 d, 70 °C), the ratio changed to 1:1.5 and the appearance of a possible third isomer was noted. Steric and ring-strain arguments suggest that the major isomers contain a five-membered ring chelating a single tungsten center, rather than spanning the W−W bond. A related cyclometalation[36] product was observed for $(silox)_3TaH_2$, which eliminates H_2 to form $(silox)_2HTa(OSi^tBu_2CMe_2CH_2)$.[5,28] On the basis of the conformation suggested by Figure 1, several rotamers possessing an asymmetric metallacycle and three distinct silox groups are plausible, but they cannot be confidently differentiated from the spectroscopic data.

When left at 25 °C for 4 h in sealed NMR tubes, **6** and free H_2 reverted to dihydride **3**. Direct reduction of $[(silox)_2WCl]_2$ (**1**) with 2.0 equiv of Na/Hg in DME also afforded **6a**, which crystallized poorly, resulting in low isolated yields (25%), whereas ^{1}H NMR spectral analysis of crude material indicated a relatively clean conversion (90%). Reduction of the dichloride (**1**) and subsequent cyclometalation was also noted when alkyllithiums (e.g., MeLi, ^{t}BuCH$_2$Li) were used in alkylation attempts.

Dihydrogen Addition to $[(silox)_2WX]_2$ (X: Cl, 1; H, 3). When significant pressures (~3 atm) of H_2 were admitted to $[(silox)_2WH]_2$ (**3**) in a sealed tube, a new hydride resonance at δ 2.67 and a single new silox peak were observed in the ^{1}H NMR spectrum (25 °C, toluene-d_8). The composition of $[(silox)_2W]_2(\mu\text{-}H)_4$ (**7**) implicated formation by oxidative addition of dihydrogen across the W≡W bond of **3**. Removal of the dihydrogen atmosphere caused an immediate reversion to **3**. The small hydride J_{WH} value of 104 Hz[37] and the 25% integrated intensity of the satellites indicated that the hydrides symmetrically bridge the two tungsten centers. The apparently high symmetry suggests a D_{2d} structure for **7**, with hydrides occupying staggered sites relative to the silox groups.[5,6]

The equilibrium between $[(silox)_2WH]_2$ (**3**) and $[(silox)_2W]_2(\mu\text{-}H)_4$ (**7**, eq 1) was measured directly by integrated intensities

$$\underset{\mathbf{3}}{(silox)_2HW{\equiv}WH(silox)_2} + H_2 \rightleftharpoons \underset{\mathbf{7}}{[(silox)_2W]_2(\mu\text{-}H)_4} \quad (1)$$

in the ^{1}H NMR over the temperature range 25.9−88.7 °C. The equilibrium constant varied between 246 and 14.2 M^{-1} in this range, and a plot of ln K_{eq} vs $1/T$ yielded thermodynamic parameters: $\Delta H° = -9.6(4)$ kcal/mol, $\Delta S° = -21(2)$ eu (1 M standard state for all species). At temperatures above ca. 70 °C, the peaks for **3**, **7**, and H_2 began to broaden simultaneously, consistent with rapid, reversible dihydrogen oxidative addition to **3**, but temperatures high enough to observe coalescence could not be reached.

Benzene solutions of $[(silox)_2WH]_2$ (**3**) under 1−3 atm of D_2 revealed incorporation of deuterium into the silox ligands, presumably via reversible cyclometalation to **6**, which occurred at an appreciable rate at 100 °C, even with competition from formation of tetrahydride **7**. Over the course of ~18 h, ^{1}H NMR spectral observation showed decreasing amounts of free HD as the concentration of H_2 increased. Isotope-shifted shoulders simultaneously appeared on the silox peak of **7**, resulting from exchange of the hydrogens initially pooled in the silox ligands for free dideuterium. Infrared analysis of **3** recovered after thermolysis under D_2 also revealed C−D stretching absorptions at 2230−2060 cm^{-1}, corroborating the NMR evidence for silox deuteration.

A related oxidative addition product was evident in low-temperature ^{1}H NMR spectra of sealed tubes containing $[(silox)_2WCl]_2$ (**1**) and dihydrogen (1−3 atm). A hydride resonance observed at δ 15.12 possessed tungsten satellites ($J_{WH} = 115$ Hz) attributed to bridging coordination (25% satellite intensity, −84 °C); hence the complex is postulated as $[(silox)_2WCl]_2(\mu\text{-}H)_2$ (**8**). The ^{1}H NMR spectrum revealed broad, overlapping silox resonances for **1** and **8**; thus the stereochemistry of the hydrido chloride is ambiguous. A plausible structure is the square-pyramid-based dimer proposed for $[(silox)_2TaCl]_2(\mu\text{-}H)_2$[5] and found for $(\eta^5\text{-}C_5H_5)_2Ta_2Cl_3R'(\mu\text{-}H)_2$ complexes prepared by Schrock *et al.*[38] The related, reversible addition of H_2 to $Cp'_2W_2Cl_4$, affording $[Cp'WCl_2]_2(\mu\text{-}H)_2$, has been reported by Green *et al.*[39] Above −60 °C (200 MHz), an exchange process obliterated the hydride and dihydrogen resonances, suggesting that addition and loss of H_2 from dichloride **1** were rapid ($\Delta G^‡ \sim 9(2)$ kcal/mol, assuming $K \sim 1$). The observation of hydrido chloride **8** raises the possibility that formation of $[(silox)_2WH]_2$ (**3**) from dichloride **1** proceeds via reduction of **8**; alternatively, **3** may be formed from a reduced intermediate derived from **1**, such as $[(silox)_2W]_2$ (**9**).

Temperature-Dependent Chemical Shifts of $[(silox)_2W]_2(\mu\text{-}H)_4$ (7). Alternative structures for $[(silox)_2W]_2(\mu\text{-}H)_4$ (**7**) include those containing terminal hydrides, provided rapid *intramolecular* scrambling of the hydride positions occurs to yield the observed ^{183}W satellite pattern indicative of μ-H ligands. Low-temperature ^{1}H NMR spectra were acquired in toluene-d_8 (≥ -70 °C), but no evidence for terminal or bridged/terminal structures was obtained. Instead, an anomalously large temperature dependence of the hydride chemical shift was found,

(35) (a) Marshall, J. L. *Carbon-Carbon and Carbon-Proton NMR Couplings*; Verlag Chemie International: Deerfield Beach, FL, 1983. (b) Leydon, D. E.; Cox, R. H. *Analytical Applications of NMR*; John Wiley & Sons: New York, 1977.

(36) For general references on cyclometalation in early transition metal systems, see: (a) Rothwell, I. P. *Polyhedron* **1985**, *4*, 177−200. (b) Rothwell, I. P. *Acc. Chem. Res.* **1988**, *21*, 153−159.

(37) Miller, R. L. Ph.D. Thesis, Cornell University, 1993.

(38) Belmonte, P. A.; Cloke, F. G. N.; Schrock, R. R. *J. Am. Chem. Soc.* **1983**, *105*, 2643−2650.

(39) Feng, Q.; Ferrer, M.; Green, M. L. H.; Mountford, P. P.; Mtetwa, V. S. B.; Prout, K. *J. Chem. Soc., Dalton Trans.* **1991**, 1397−1406.

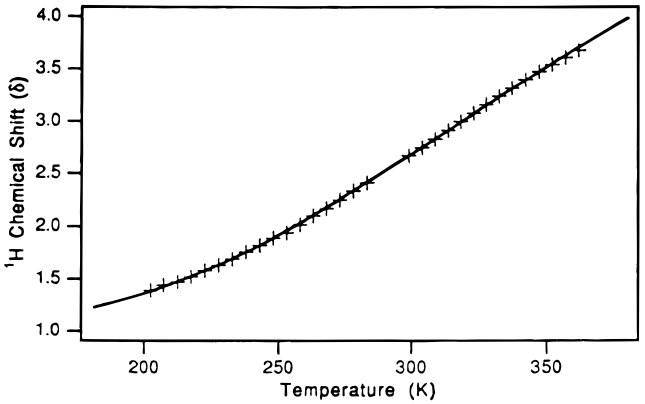

Figure 2. Temperature dependence of the hydride ^{1}H NMR chemical shift of $[(silox)_2W]_2(\mu\text{-}H)_4$ (**7**). The data were fit as shown by the strong antiferromagnetic coupling model according to eq 2 (δ_{dia} 1.04, A = 0.536 MHz, $-2J = -873.7$ cm^{-1}). A similar fit was obtained using the diamagnetic equilibrium model as expressed in eq 6 (δ_{7a} 1.15, δ_{7b} 7.49, $\Delta H° = 2.6$ kcal/mol, $\Delta S° = 6.3$ eu).

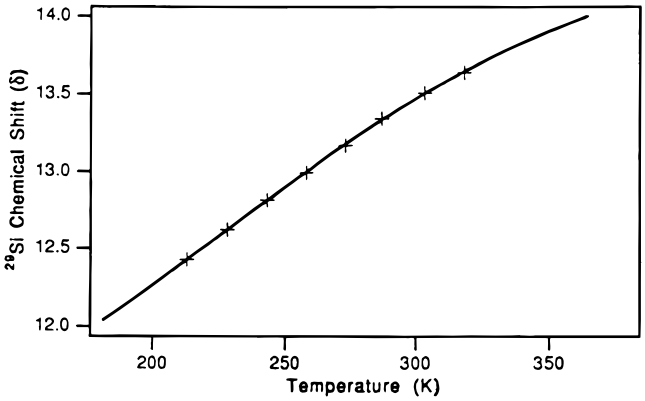

Figure 3. Temperature dependence of the silox ^{29}Si chemical shift of $[(silox)_2W]_2(\mu\text{-}H)_4$ (**7**). The data were fit as shown by the strong antiferromagnetic coupling model according to eq 2 (δ_{dia} 11.51, A = 0.082 MHz, $-2J = -616.6$ cm^{-1}). A similar fit was obtained using the diamagnetic equilibrium model as expressed in eq 6 (δ_{7a} 11.79, δ_{7b} 15.21, $\Delta H° = 2.1$ kcal/mol, $\Delta S° = 6.9$ eu).

varying from δ 1.39 (−70 °C), to δ 3.68 (90 °C). The chemical shift, determined at 5 °C intervals in this range, is plotted in Figure 2. Below −70 °C, the resonance overlapped with silox signals and could not be detected, and above 90 °C, rapid exchange with H_2 caused additional shift deviations.

Sharp hydride and silox resonances indicated a diamagnetic ground state, but the slightly sigmoidal chemical shift temperature dependence may reflect the presence of a low-lying paramagnetic excited state.[40−42] The W═W bond of **7** may be described as $\sigma^2\delta^2$ ($^1A_1$ ground state), with energetically nearby triplet states of the $\delta\delta^*$ type ($^3B_1$, $^3B_2$).[32,41] EHMO and *ab initio* calculations were conducted in order to explore the validity of such electronic descriptions. In an attempt to directly assess the concentration of paramagnetic entities, Evans' method[40] measurements were conducted on solutions containing **3**, H_2, and **7**, but the estimated solvent (C_6D_5H) shift (0.9 Hz) based on a singlet−triplet splitting of $\Delta E = 745$ cm^{-1} (*vide infra*) was unfortunately well within its experimental line width (5.5 Hz). In an effort to corroborate this interpretation of the shift dependence, variable-temperature ^{29}Si{^{1}H} NMR spectra of **7** were also studied between −60 and +45 °C. The chemical shift of the silox ^{29}Si signal (Figure 3) varies between δ 12.43 and 13.64 before it broadens due to rapid interconversion with $[(silox)_2WH]_2$ (**3**) via H_2 loss.

Discussion

Tungsten Silox Hydrides. Inclusion of silox (X) in the coordination sphere of prototypical $X_2YW{\equiv}WX_2Y$ species has permitted the synthesis of discrete dinuclear hydride (Y) complexes. The added steric bulk of the tri-*tert*-butylsilyl group prevents aggregation of $[(silox)_2WH]_2$ (**3**) and its related hydrides, a common phenomenon exemplified in the formation of $[W_2(\mu\text{-}H)(O^iPr)_7]_2$[18] and $W_6(\mu\text{-}H)_4(\mu\text{-}O^iPr)_7(\mu\text{-}C^iPr)(H)(O^iPr)_5$.[19] Additional bases are not needed to stabilize dimeric hydride species (cf. $W_2H_2(O^iPr)_6(dmpe)_2$),[19] thereby retaining the hexacoordination sphere of the metal−metal triple bond. Significant deviation from classical staggered geometries[30−32] is considered to arise from the steric influence of silox (Figure 1), but X-ray structural confirmation of the proposed distortions has remained elusive.

Noting that $K_{eq} \sim 1$ for both the ethylene insertion (**3** + $2H_2C{=}CH_2 \rightleftharpoons$ **5**)) and H_2 elimination/cyclometalation (**3** $\rightleftharpoons$ **6** + H_2) reactions (Scheme 1), attempts to roughly calculate $\{D(W-H) - D(W-C)\}$ were made using standard thermochemical data and crude estimates of $\Delta S°$.[44] Unreasonable, disparate answers were obtained for the two reactions, indicating that the assumption intrinsic to the analyses—that the $[(SiO)_2W]_2$ core remains relatively unperturbed during each transformation—was probably naive. Many contributing factors are difficult to estimate: the degree of distortion from the gauche or anti conformers in each complex, the enthalpic contribution from ring formation upon metalation, entropic contributions unique to this system, etc. Since irreversible ethylene insertions into tantalum hydrides $[(silox)_2TaH_2]_2$ and $[(silox)_2TaH]_2(\mu\text{-}O)_2$ have been observed,[5] it is likely that $\{D(W-H) - D(W-C)\} > \{D(Ta-H) - D(Ta-C)\}$ as expected.[45] The ability of silox to electronically and sterically compensate for structural and coordination changes must allow it to mitigate reactivity about the W≡W bond.

Modeling the Temperature-Dependent Chemical Shifts of $[(silox)_2W]_2(\mu\text{-}H)_4$ (7). Complexes displaying strong antiferromagnetic coupling between two or more transition metal centers often manifest chemical shift temperature dependencies.[41] Observation by NMR spectroscopy does not require analytically pure material and is relatively insensitive to paramagnetic impurities, because it probes local magnetic effects.[46] Since H_2 loss from $[(silox)_2W]_2(\mu\text{-}H)_4$ (**7**) prevents its isolation as a solid and equilibrium amounts of **3** are always present, NMR analysis presents obvious advantages to bulk susceptibility measurements.

(40) (a) Campbell, G. C.; Haw, J. F. *Inorg. Chem.* **1988**, *27*, 3706−3709. (b) Campbell, G. C.; Reibenspies, J. H.; Haw, J. F. *Inorg. Chem.* **1991**, *30*, 171−177. (c) Walter, T. H.; Oldfield, E. *J. Chem. Soc., Chem. Commun.* **1987**, 646−647.

(41) (a) Cotton, F. A.; Eglin, J. L.; Hong, B.; James, C. A. *Inorg. Chem.* **1993**, *32*, 2104−2106. (b) Cotton, F. A.; Eglin, J. L.; James, C. A.; Luck, R. L. *Inorg. Chem.* **1992**, *31*, 5308−5315. (c) Cotton, F. A.; Eglin, J. L.; Hong, B.; James, C. A. *J. Am. Chem. Soc.* **1992**, *114*, 4915−4917.

(42) Kriley, C. E.; Fanwick, P. E.; Rothwell, I. P. *J. Am. Chem. Soc.* **1994**, *116*, 5225−5232.

(43) (a) Evans, D. F. *J. Chem. Soc.* **1959**, 2003−2005. (b) Orrell, K. G.; Sik, V. *Anal. Chem.* **1980**, *52*, 567−569.

(44) (a) Benson, S. W. *Thermochemical Kinetics*; John Wiley & Sons: New York, 1968. (b) Carpenter, B. K. *Determination of Organic Reaction Mechanisms*; John Wiley & Sons: New York, 1984.

(45) Schock, L. E.; Marks, T. J. *J. Am. Chem. Soc.* **1988**, *110*, 7701−7715 and references therein.

(46) (a) Boersma, A. D.; Phillippi, M. A.; Goff, H. M. *J. Magn. Reson.* **1984**, *57*, 197−203. (b) Holm, R. H.; Hawkins, C. J. In *NMR of Paramagnetic Molecules*; La Mar, G. N., Horrocks, W. DeW., Holm R. H., Eds.; Academic: New York, 1973; Chapter 7. Values of physical constants: $|\gamma_e| = 1.761 \times 10^7$ s^{-1} G^{-1}; $|\gamma_H| = 2.675 \times 10^4$ s^{-1} G^{-1}; $|\gamma_{Si}| = 5.316 \times 10^3$ s^{-1} G^{-1}.

The expression for the temperature dependence of the chemical shift, δ_{obs}, of a singlet species with a low-lying triplet excited state is given by[46]

$$\delta_{obs} = \delta_{dia} + \frac{2|\gamma_e|A}{|\gamma_N|kT}(3 + e^{2J/kT})^{-1} \quad (2)$$

In eq 2, δ_{obs} is the observed chemical shift, A is the triplet state electron−nuclear hyperfine coupling (in MHz), and $-2J$ is the singlet−triplet energy separation, typically expressed in cm^{-1}. δ_{dia} is the chemical shift the observed nucleus would exhibit in an equivalent diamagnetic environment; in some cases an appropriate diamagnetic model exists, but usually δ_{dia} is treated as an unknown, and was in this instance. The magnitude of the deviation in chemical shift is dependent on the relative magnetogyric ratios of the free electron ($|\gamma_e|$) and the nucleus under observation ($|\gamma_N|$) and on the hyperfine coupling constant, A.

Nonlinear, least-squares fits to eq 2 yielded the parameters listed in Figure 2, with each fit shown superimposed on the temperature-dependent ^1H and $^{29}Si\{^1H\}$ shifts. An alternate, rejected solution gave $-2J = -215\ cm^{-1}$, a splitting considered too small to produce the observed narrow NMR lines (e.g., $\nu_{1/2}(W_2H) \sim 5$ Hz), assuming the susceptibility of **7*** is not greatly attenuated via spin−orbit and related effects. Comparing the parameters obtained from the ^{29}Si and ^1H NMR spectra, the values of δ_{dia} and A are plausible, but the agreement between $-2J$ values −873.7 and -616.6 cm^{-1} is poor, however probably within the range of error expected for this rough model. Equation 2 assumes a contact-shift model for the paramagnetism that does not accommodate minor effects from diamagnetic anisotropy associated with the metal−metal multiple bond[32] or other distance-dependent effects. These effects are impossible to quantify without a detailed knowledge of the structure of **7**. Since through-space contributions decrease as $1/r^3$, the more distant nucleus (^{29}Si) should give more accurate parameters.[41] Unfortunately, the experimental temperature and shift ranges for ^{29}Si were somewhat abbreviated; hence no preference for either set of fitting parameters is espoused. Taking an average of the $-2J$ values (745 cm^{-1}), the paramagnetic excited state is roughly 2.1 kcal/mol above the ground state.

An alternative to the low-lying excited state model was also investigated. Consider an equilibrium between two structural isomers in rapid exchange (**7a** ⇌ **7b**). If the equilibration involves a bridge-for-terminal hydride exchange (e.g., $[(silox)_2W]_2(\mu\text{-}H)_4$ (**7a**, **A**) ⇌ $[(silox)_2WH_2]_2$ or $[(silox)_2WH]_2(\mu\text{-}H)_2$ (**7b**, **B**),[47] then the corresponding $\Delta G^{\ddagger}$ must be less than ∼9 kcal/mol for the tungsten satellites to remain sharp at temperatures as low as −70 °C. Silox ligand rearrangement must be minimal (cf. $[(silox)_2TaH]_2(\mu\text{-}H)_2(\mu\text{-}O)$),[5] or else the barrier would be higher and some indication of coalescence would be observed. The simplest model assumes that each isomer, **A** and **B**, can be represented by a single (time-averaged) ^1H NMR hydride shift, δ_A and δ_B, respectively. Recalling that the observed shift is the mole fraction-weighted average $\delta_{obs} = \chi_A\delta_A + \chi_B\delta_B$ and that $\chi_B/\chi_A = K_{eq} = \exp(-\Delta G°/RT)$, it is possible to derive an expression for the temperature dependence of the chemical shift in a rapidly exchanging system (eqs 3−6).

$$\exp(-\Delta G°/RT) = \chi_B/\chi_A = (1 - \chi_A)/\chi_A = (1/\chi_A) - 1 \quad (3)$$

$$\chi_A = 1/\{1 + \exp(-\Delta G°/RT)\} \quad (4)$$

$$\delta_{obs} = \chi_A(\delta_A - \delta_B) + \delta_B \quad (5)$$

$$\delta_{obs} = \frac{\delta_A - \delta_B}{1 + \exp(-\Delta G/RT)} + \delta_B \quad (6)$$

Four-parameter fits of the ^1H and ^{29}Si shifts of **7** to eq 6 had broad regions of minimization, but global minima were found with the parameters listed in the captions in Figures 2 and 3. The predicted chemical shifts for the hydrides and siloxes of **7a**/**7b** lie within plausible ranges,[47] and the agreement between the free energy parameters derived from the independent fits is somewhat better than the previous model. The free energies that arise from the fits (298 K: ^1H, $\Delta G° \sim 0.69$ kcal/mol; ^{29}Si, $\Delta G° \sim 0.035$ kcal/mol) suggest that the higher energy structure might be directly observed by IR, but significant hydrogen pressures are necessary to ensure formation of **7** without substantial $[(silox)_2WH]_2$ (**3**) present; high-pressure IR studies were not attempted.

While both treatments provide plausible explanations for the observed temperature-dependent hydride and silox silicon chemical shifts, the thermally accessible excited state is slightly favored. Recall that the J_{WH} of 104 Hz is insensitive to the temperature change. A diamagnetic isomer in thermal equilibrium (e.g., with $\Delta G° \sim 0.69$ kcal/mol, χ(**7b**) ∼ 0.25) that contains terminal and bridging hydrides would have to possess nearly the same average J_{WH}. This prospect is somewhat unlikely since terminal hydrides in this system have couplings >300 Hz and an average bridging hydride $J_{W2H} \sim 108$ Hz.[37] In contrast, fractional population of an excited state ($\Delta G° \sim$ 2.1 kcal/mol, χ(**7***) ∼ 0.03) would be unlikely to change the coupling constant, especially since the putative $\delta\delta$* excited state should not manifest much of a structural change from the ground state species (*vide infra*).

It is also interesting to note that related excited states are the cornerstone of several similar treatments pertaining to W_2 quadruple-bonded complexes,[41] where the $\delta\delta$* singlet state lies ∼11 000 cm^{-1} above the ground state. In cases where an estimate of the $\delta\delta$* triplet state is available via temperature-dependent ^{31}P chemical shift measurements, it lies only ∼2000 cm^{-1} above the ground state. The similarity of the orbitals involved provides precedence that low-lying triplet states ($^3B_1$ and $^3B_2$) are present and influencing the ^1H and ^{29}Si chemical shifts of **7**.

Extended Hückel Calculations on $(silox)_4M_2H_4$. In order to assess the metal−hydride and metal−metal bonding in the putative D_{2d} structure of $[(silox)_2WH_2]_2$ (**7**), extended Hückel molecular orbital (EHMO)[48] calculations were conducted on the model complex $(H_3SiO)_4W_2H_4$ (**7′**). The lack of core repulsion terms in the extended Hückel method makes geometry optimizations unreliable, so the postulated structure of the $W_2(\mu\text{-}H)_4$ core in **7′** was based on neutron diffraction data for $Ta_2Cl_4(PMe_3)_4(\mu\text{-}H)_4$[6] and $Re_2H_4(PEt_2Ph)_4(\mu\text{-}H)_4$.[49] Metal−metal bond distances in these structures (2.511 and 2.538 Å, respectively) appear to be dominated by the requirements of the μ-H bridges rather than the metal d-electron counts.

Several other conformations of $[(silox)_2WH_2]_2$ (**7**) are possible, including a D_{2h} arrangement where the Si−O−W linkages lie in a single plane, as opposed to two orthogonal planes of a D_{2d} arrangement. The plausibility of eclipsed silox groups in the D_{2h} structure was explored via molecular mechanics calculations on the $W_2(silox)_4$ unit at various fixed W−W

(47) For binuclear hydrides with terminal sites upfield of bridging, see: Fryzuk, M. D.; McConville, D. H. *Inorg. Chem.* **1989**, *28*, 1613−1614. Green, M. A.; Huffman, J. C.; Caulton, K. G. *J. Am. Chem. Soc.* **1982**, *104*, 2319−2320. Green, M. A.; Huffman, J. C.; Caulton, K. G. *J. Am. Chem. Soc.* **1981**, *103*, 695−696.

(48) Hoffmann, R. *J. Chem. Phys.* **1963**, *39*, 1397−1412.

(49) Bau, R.; Carroll, W. E.; Teller, R. G.; Koetzle, T. F. *J. Am. Chem. Soc.* **1977**, *99*, 3872−3874.

distances. In both configurations, the tungstens and oxygens were held fixed, as were the W−O distances, while the rest of the molecule was allowed to optimize freely. At a W−W distance of 2.5 Å, the molecule encounters a barrier to eclipsing of the silox groups of 37 kcal/mol. The relatively short d(W−W) ∼ 2.52 Å expected for hydride-bridged ditungsten species,[50] in combination with the molecular mechanics results, leads to the practical exclusion of structures possessing eclipsed silox ligands.

Two possible geometries of four equivalent bridging hydrides about a D_{2d} W_2(silox)$_4$ unit were considered: one symmetric case with the (μ-H) unit rotated 45° relative to the silox ligands and another with the hydrides eclipsing the W−O vectors. The eclipsed configuration was calculated to be 1.04 eV (∼24 kcal/mol) higher in energy than the staggered case, leading to its exclusion from further consideration.[51] The higher energy in the eclipsed configuration is a direct consequence of a destabilizing trans influence of the silox group.

The molecular orbitals corresponding to [$(H_3SiO)_2W]_2(\mu$-H)$_4$ (**7a′**), which models the putative D_{2d}, staggered-μ-hydride structure of **7**, are composed from the interaction of H_4 fragment molecular orbitals (FMOs) with those of D_{2d} [$(H_3SiO)_2W]_2$ (**9′**). As Figure 4 illustrates, assembling **9′** via interaction of the well-known frontier molecular orbitals of two C_{2v} ML_2 (e.g., ($H_3SiO)_2W$) fragments[52] results in five low-lying metal−metal bonding orbitals and five corresponding antibonding orbitals. As a consequence of the low coordination geometry and π-type molecular orbitals (e) that arise from the combination of a low-lying d_{xz} (d_{yz}) of one $(H_3SiO)_2W$ with a high-lying d_{xz} (d_{yz}) of another, a stable L_4M_2 complex possessing a quintuple metal−metal bond (d^5−d^5; $\sigma^2\pi^4\delta(d_{x^2-y^2})^2\delta(d_{xy})^2$) is theoretically possible. Both the $d_{x^2-y^2}$ and d_{xy} orbitals have δ-overlap in this configuration, but the $d_{x^2-y^2}$ bonding combination is further stabilized by δ-σ mixing allowed in D_{2d} symmetry; hence it is the HOMO for d^4−d^4 **9′**, which exhibits the classic $\sigma^2\pi^4\delta^2$ ordering accorded a formal quadruple bond. The composition of the HOMO is 55% $d_{x^2-y^2}$, 38% d_{z^2}, and 7% s. The net result of the 45% σ-contribution to the HOMO is a reduction of the lobes of the W $d_{x^2-y^2}$ that point toward the siloxide ligands and reinforcement of those directed away, effectively buffering its energy to small O−W−O angular changes.

The diagram depicting the interaction of [$(H_3SiO)_2W]_2$ (**9′**) with the staggered H_4 FMOs is shown on the left side of Figure 5. The FMOs of the H_4 unit are substantially split due to their relatively close interaction (d(H···H) = 1.98 Å).[49] The hydride FMOs have the correct symmetry ($a_1 + b_1 + e$) to interact with four of the W−W bonding levels in **9′**. The metal $\delta(b_1)$ and π(e) sets are pushed high up in energy by this interaction, while the energy of the σ (a_1) rises only slightly due to a stabilizing, second-order interaction with the $d_{x^2-y^2}$-based δ^* (a_1) orbital. After interaction with the hydrides, the tungsten centers are now formally d^2, leading to an $(a_1)^2(b_2)^2$ configuration and a formal W═W double bond ($\sigma^2\delta^2$). The LUMO is the d_{xy}-based δ^* (a_2) orbital, while the HOMO (principally $d_{x^2-y^2}$) is virtually the same as in **9′**; thus the 0.63 eV HOMO−LUMO gap reflects a δ−δ^* separation between two distinct δ-type interactions. A second δ-δ^* separation of 0.93 eV arises from the a_1 LUMO+1 (δ^*) comprising the antisymmetric combination of the $d_{x^2-y^2}$ orbitals, including a significant amount of σ-contribution.

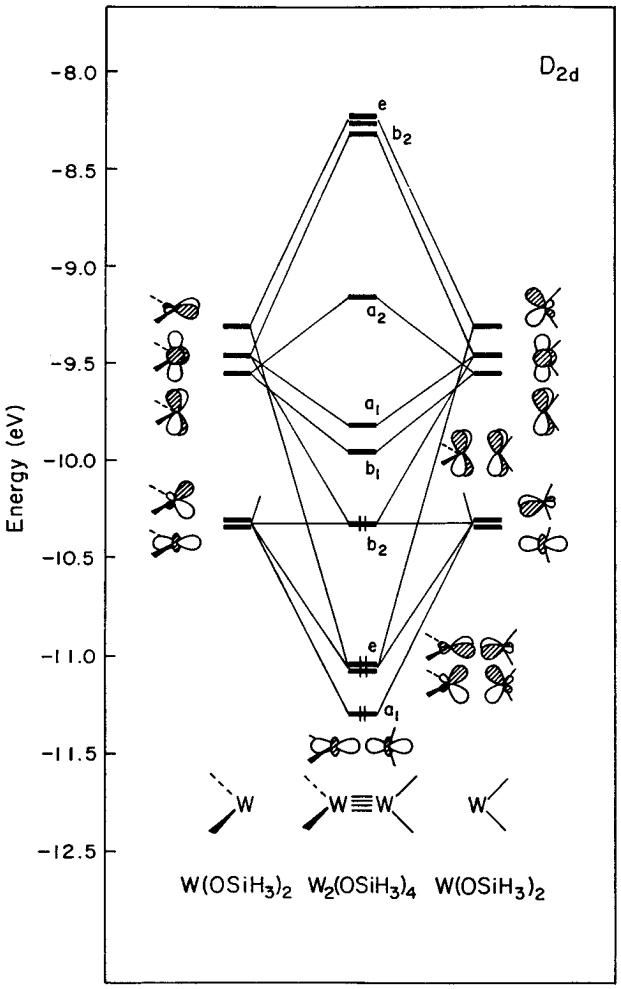

Figure 4. Molecular orbital diagram of D_{2d} [$(H_3SiO)_2W]_2$ (**9′**), a model of putative [$(silox)_2W]_2$ (**9**), as determined from an EHMO calculation: d(W−W) = 2.25 Å, d(W−O) = 1.88 Å, d(Si−O) = 1.68 Å, d(Si−H) = 1.47 Å, ∠W−W−O = 115°, ∠W−O−Si = 180°.

For comparison, the molecular orbital diagram for [(H_3-$SiO)_2WH_2]_2$ (**7b′**) with all-terminal, axial hydrides (∠WWH = 90°) is depicted on the right side of Figure 5. The hydrides lie in the same plane as the distal WO_2 unit and transform as $a_1 + b_2 + e$ in D_{2d} symmetry, with the H_4 FMOs manifesting little splitting due to the large interatomic distances. The a_1 and b_2 hydride levels are stabilized significantly, as the $W_2(OSiH_3)_4$ (**9′**) δ^* (a_1) and δ (b_2) FMOs have large lobes pointing toward the apical sites on the metal centers. The b_2 and a_1 W−W orbitals are destabilized significantly, but the π (e) set is destabilized to only a minor extent due to poor overlap with the axial hydrides. Little M−H bonding character is present in the H_4 localized e set; hence, while **7b′** formally contains four W−H bonding orbitals, two are essentially nonbonding. As a consequence, the net stabilization of the H_4 FMOs in the all-terminal structure is weak in comparison to that of the all-bridged geometry. Inspection of the diagram reveals that the HOMO of **7b′** is the half-occupied e (π) set, suggesting that the ground state of an all-terminal hydride conformation would be a triplet. The lack of substantial stabilization needed for four terminal W−H bonds and the implication of a triplet ground state indicate that the all-terminal hydride structure is a poor model for [$(silox)_2WH_2]_2$ (**7**). Note that the ground state structural preference in the related singly bonded [$(silox)_2TaH_2]_2$[5] is less straightforward. In this d^1−d^1 derivative, the lack of a

(50) (a) Bau, R.; Carroll, W. E.; Hart, D. W.; Teller, R. G.; Koetzle, T. F. *Adv. Chem. Ser.* **1978**, *167*, 73−92. (b) Bau, R.; Teller, R. G.; Kirtley, S. W.; Koetzle, T. F. *Acc. Chem. Res.* **1979**, *12*, 176−183.

(51) Previous calculations carried out on hydrido-bridged transition metal dimers yield similar results for different modes of ligand rotation about the M−M bond: Dedieu, A.; Albright, T. A.; Hoffmann, R. *J. Am. Chem. Soc.* **1979**, *101*, 3141−3151.

(52) Albright, T. A.; Burdett, J. K.; Whangbo, M.-H. *Orbital Interactions in Chemistry*; John Wiley & Sons: New York, 1985.

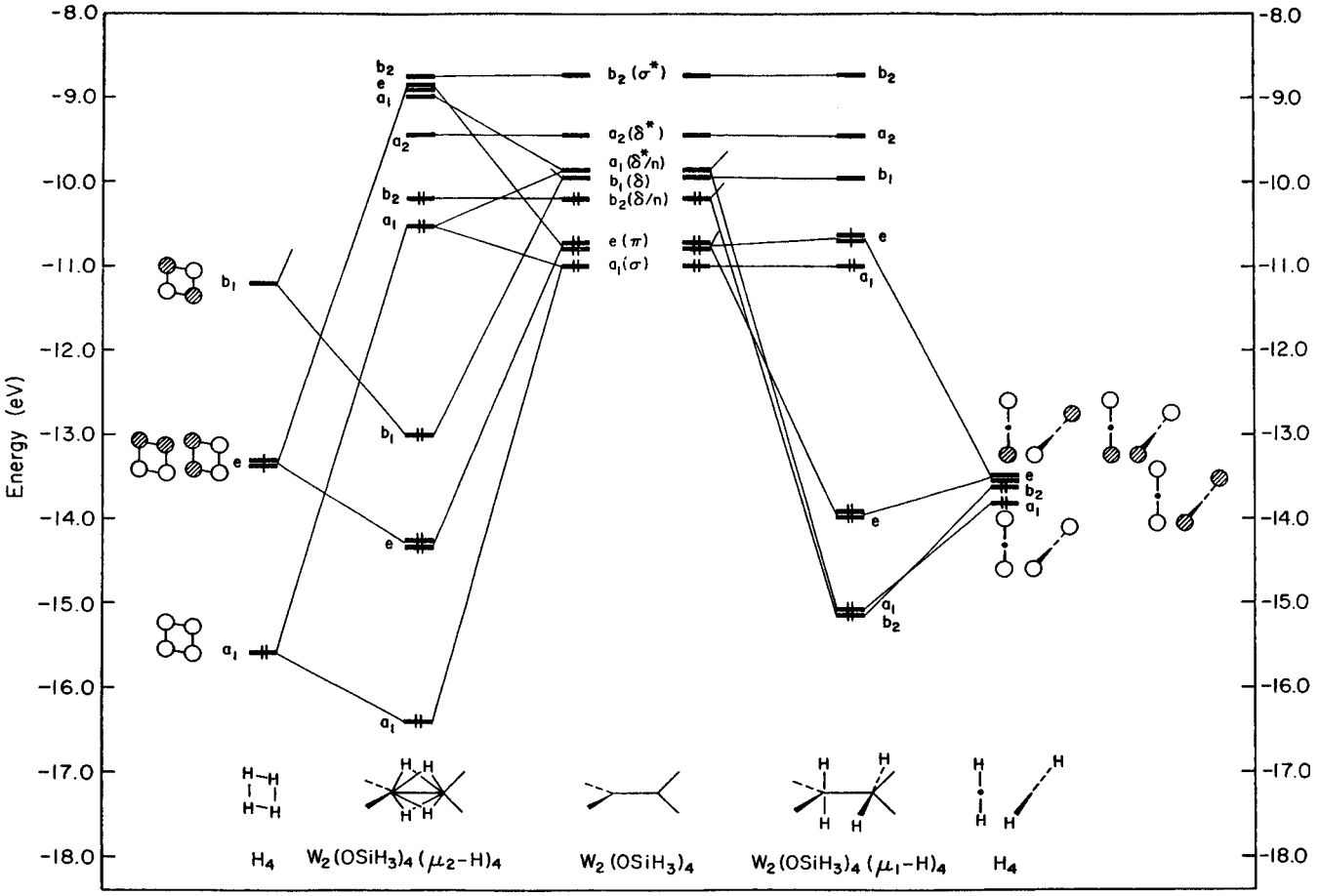

Figure 5. Molecular orbital diagram of bridged, D_{2d} $[(H_3SiO)_2W]_2(\mu\text{-}H)_4$ (**7a′**), a model of $[(silox)_2W]_2(\mu\text{-}H)_4$ (**7a**), and all-terminal, D_{2d} $[(H_3SiO)_2WH_2]_2$ (**7b′**), a model of $[(silox)_2WH_2]_2$ (**7b**), as determined from EHMO calculations: d(W−W) = 2.45 Å, d(W−O) = 1.88 Å, d(Si−O) = 1.68 Å, d(Si−H) = 1.47 Å, d(W−H_{bridge}) = 1.88 Å, d(W−H_{term}) = 1.68 Å, ∠W−W−O = 120°, ∠W−O−Si = 180°.

Ta−Ta δ-bonding interaction undoubtedly helps skew the D_{2d} complex toward the all-terminal form, with a comparatively lengthy (2.72 Å) Ta−Ta distance.

***Ab Initio* Calculations on $[(silox)_2WH_2]_2$ (7).** The EHMO calculations do not provide an accurate comparison of the energies of alternative structures, in part because the total energy depends greatly on the choice of W−H bond lengths, which cannot be optimized. In order to assess the plausibility of a staggered $[(silox)_2W]_2(\mu\text{-}H)_4$ (**7**) structure that possesses a singlet ground state and a thermally accessible triplet excited state, a higher level of computation was employed. Using an extremely simple model complex, $(HO)_4W_2(H_4)$ (**7″**), *ab initio* calculations that utilized effective core potentials on the tungstens[53] were performed at the restricted Hartree−Fock (RHF) level. Geometry optimizations started from a symmetrically bridged model, $[(HO)_2W]_2(\mu\text{-}H)_4$ (**7a″**), and retained only S_4 symmetry so the hydrides could bend back and rotate into a variety of terminal and bridging configurations. The minimum-energy configuration under these constraints was found to be the symmetrically bridged structure with the following bond distances and angles: d(W−W) = 2.50 Å, d(W−O) = 1.87 Å, d(W−H) = 1.89 Å, ∠WWH = 48.6°.

Unrestricted Hartree−Fock (UHF) optimization of a triplet species retaining S_4 symmetry yielded a structure with "bent-terminal" or "semibridging" hydrides. The UHF-optimized structural model places each hydride 1.72 and 2.28 Å from proximal and distal tungsten atoms, respectively; the tungstens are 2.58 Å apart and the accompanying W−W−H angle is 40.9°. Each hydride is also coplanar with its distal WO_2 unit, as in the all-terminal structure, but no significant destabilization occurs as the W_{dist}−H and W−O bond distances are longer than in **7b′**. Electronic factors favor this arrangement by ∼3 eV (EHMO) relative to the symmetric eclipsed alternative. As expected, the longer W−W bond distance that results from population of a W−W antibonding orbital in the excited state (triplet) configuration. Rotation of the H_4 unit to access a semibridged structure containing hydrides eclipsing proximal silox groups encounters a severe (∼5−6 eV depending on d(W−W), EHMO) barrier due to steric and electronic factors.

The semibridging/bent-terminal structure for triplet **7″** is most easily interpreted by returning to the extended Hückel method, using geometries obtained from *ab initio* calculations. Figure 6 illustrates a correlation diagram for the all-terminal and "semibridged" structures. The a_1 W−H bonding level low in energy is stabilized, and the b_2 W−H bonding level is somewhat destabilized, but now the e hydride set exhibits significant stabilization. By bending toward the distal metal, the H's can overlap with the large lobes of the W−W π-bonding FMOs, allowing the formation of four W−H bonding orbitals rather than just the two manifested by the all-terminal structure. It is also pertinent to note that the hydrides are considerably further apart in the semibridged geometry. In related $Ta_2Cl_4(PMe_3)_4(\mu\text{-}H)_4$[6] and $Re_2H_4(PEt_2Ph)_4(\mu\text{-}H)_4$[49] complexes, the remaining four ligands on each metal help force the hydrides close together, but $[(silox)_2WH_2]_2$ (**7**) possesses only two silox groups per tungsten, making it possible for deviation to the semibridged form.

(53) (a) Stevens, W. J.; Basch, H.; Krauss, M. *J. Chem. Phys.* **1984**, *81*, 6026−6033. (b) Stevens, W. J.; Basch, H.; Krauss, M.; Jasien, P. *Can. J. Chem.* **1992**, *70*, 612−630.

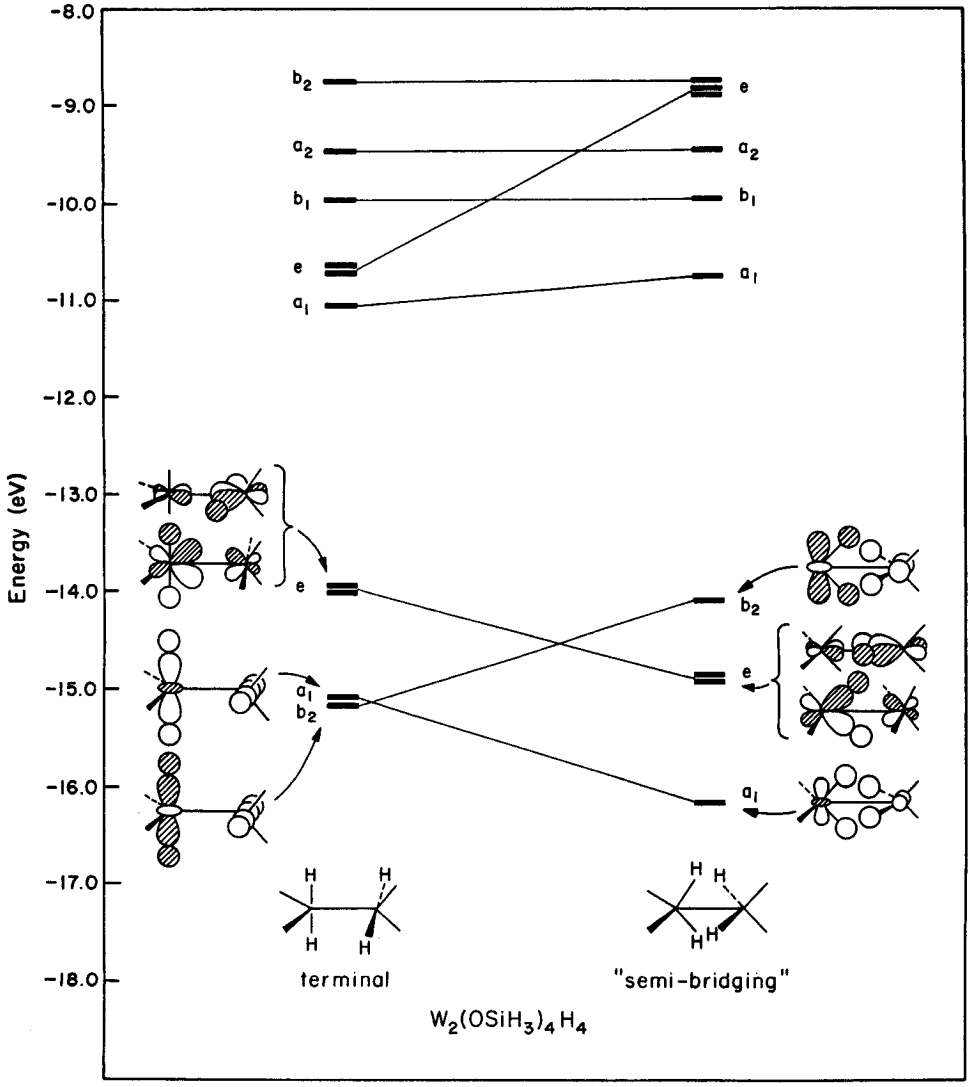

Figure 6. Molecular orbital diagram of semibridged, D_{2d} $[(H_3SiO)_2WH_2]_2$ (**7″**), a model relevant to the excited state of putative $[(silox)_2W]_2(\mu\text{-H})_4$ (**7a**), as determined from an EHMO calculation used to highlight the results of an ab initio calculation: d(W−W) = 2.45 Å, d(W−O) = 1.88 Å, d(Si−O) = 1.68 Å, d(Si−H) = 1.47 Å, d(W−$H_{semibridge}$) = 1.68 Å, d(W−H_{term}) = 1.68 Å, ∠W−W−O = 120°, ∠W−O−Si = 180°.

The *ab initio* results still contain ambiguities that might be resolved at even higher levels of theory. Nonetheless, these preliminary calculations, in conjuction with the EHMO results, give credence to the postulated symmetric, staggered $[(silox)_2W]_2(\mu\text{-H})_4$ ground state structure for **7**. A low-lying triplet excited state with a semibridging geometry is plausible, and the structural change that accompanies bond lengthening aids in rationalizing the small singlet−triplet gap implicated experimentally. If a thermally accessible triplet state is "semibridged", the hydrides are still coupled to both tungstens, and rapid interconversion of the hydrides should yield average J_{W2H} values similar to those of the symmetric ground state. A series of semibridged $[(silox)_2W]_2(\mu\text{-H})_2(\mu\text{-RC}{\equiv}\text{CR})$ derivatives exhibited average coupling constants in the 104−110 Hz range.[37] For a relevant system, Bau *et al.* concluded that the terminal and bridging hydrides of $Re_2H_4(PEt_2Ph)_4(\mu\text{-H})_4$ exchange rapidly.[49]

Putative [(silox)$_2$W]$_2$. A discrete D_{2d}, quadruply bonded intermediate, $(silox)_2W\overset{4}{—}W(silox)_2$ (**9**), has been alluded to as a possible source of chemistry subsequent to the reduction of $[(silox)_2WCl]_2$ (**1**). For example, its existence would provide a ready pathway for cyclometalation to give $(silox)_2HW{\equiv}W(OSi^tBu_2CMe_2CH_2)(silox)$ (**6a**). Jones *et al.* have prepared $[(^tBu_2P)Mo]_2(\mu\text{-}P^tBu_2)$,[54] but the propensity of phosphides to bridge makes this a rather dubious model for the putative siloxide species, **9**. While evidence for **9** is circumstantial, EHMO calculations on **9′** (Figure 4) reveal that enhanced reactivity should be expected relative to coordinatively saturated $M_2L_8^{n-}$ counterparts.[32] An estimate of its W_2 bond order is obtained by comparing the calculated Mulliken overlap population of 1.196 to those of other structurally characterized quadruple bonds. $W_2Cl_4(PMe_3)_4$[55] (modeled as $W_2Cl_4(PH_3)_4$) and $[W_2Me_8]^{4-}$ [56] have overlap populations of 1.114 and 1.232, respectively. Formally a $\sigma^2\pi^4\delta^2$ configuration, the quadruple bond of $(H_3SiO)_4W_2$ partitions into 37% σ, 58% π, and only 5% δ overlap. The small δ contribution stems from the aforementioned $\sigma-\delta$ mixing allowed in D_{2d} symmetry (but not in D_{4d}), which increases the stabilization of the δ (b_2) orbital but also reduces its relative δ contribution. The b_1 LUMO, composed of pure δ overlap, is slightly more bonding than the HOMO.

The reactivity of d^4-d^4 M_2L_8 complexes such as $W_2Cl_4(PMe_3)_4$ and $[W_2X_8]^{4-}$ (X = Cl, Me) is dominated by simple ligand substitutions that leave the metal−metal bond intact[57] and by severe oxidative processes involving halogens, dichal-

(54) Jones, R. A.; Lasch, J. G.; Norman, N. C.; Whittlesey, B. R.; Wright, T. C. *J. Am. Chem. Soc.* **1983**, *105*, 6184−6185.
(55) Cotton, F. A.; Felthouse, T. R.; Lay, D. G. *J. Am. Chem. Soc.* **1980**, *102*, 1431−1433.
(56) Collins, D. M.; Cotton, F. A.; Koch, S. A.; Millar, M.; Murillo, C. A. *Inorg. Chem.* **1978**, *17*, 2017−2021.

cogenides, or alkyl iodides.[58] In contrast, putative D_{2d} $(silox)_4W_2$ (**9**) is inferred to be a potent reductant for H−H and intramolecular C−H bonds. The formal relationship between **9** and the M_2L_8 complexes involves the binding of four additional donor ligands; thus the high reactivity of $(silox)_4W_2$ is considered to be a direct result of its coordinative unsaturation. The large lobes of the δ^* (a_1) LUMO+1 orbital are directed at the vacant axial sites and should be good acceptors for any approaching substrate electron pair, either a lone pair or a σ- or π-bond. With the approach of a substrate, the δ (b_2) orbital is destabilized. The filled δ (b_1) orbital (now the HOMO) has appropriate symmetry to strongly back-donate into σ^* (H−H or C−H) orbitals during the course of oxidative addition. Further reactivity studies of putative $(silox)_4W_2$ (**9**), including trapping attempts with various donors, are underway.

Experimental Section

General Considerations. All manipulations were performed using either glovebox or high-vacuum-line techniques. Ethereal solvents, and hydrocarbon solvents containing 1−2 mL of added tetraglyme, were distilled under nitrogen from purple sodium benzophenone ketyl and vacuum-transferred from same prior to use. Benzene-d_6 was dried over activated 4 Å molecular sieves, vacuum-transferred, and stored under N_2; toluene-d_8, methylcyclohexane-d_{14}, and THF-d_8 were dried over sodium benzophenone ketyl. All glassware was oven-dried, and NMR tubes were also flame-dried under dynamic vacuum. H_2 and D_2 were passed over activated MnO and 4 Å sieves. WCl_4 was prepared from WCl_6 and $W(CO)_6$[59] (Aldrich), which were used as received.

NMR spectra were obtained using Varian XL-200, XL-400, VXR-400S, and Bruker AF-300 spectrometers. Probe temperatures were calibrated using methanol and ethylene glycol standards. Chemical shifts are reported relative to TMS, and all nonlinear least-squares fits were carried out using Igor (WaveMetrics). Infrared spectra were recorded on a Mattson FT-IR interfaced to an AT&T PC7300 computer or on a Perkin Elmer 299B spectrophotometer. Elemental analyses were performed by Texas Analytical Laboratories, Houston, TX, or Oneida Research Services, Whitesboro, NY. Molecular weights were determined by benzene cryoscopy on a home-built device.

Preparations. 1. $[(silox)_2WCl]_2$ (1). Into a 250 mL, three-neck flask charged with WCl_4 (3.23 g, 9.92 mmol) and equipped with a solids-addition tube containing 0.9% Na/Hg (25.4 g, 9.9 mmol), was distilled 100 mL of THF at −78 °C. A portion of the amalgam was added to the vigorously stirred black slurry at −78 °C, and the mixture was allowed to warm to 25 °C. After 1 h, the remaining amalgam was added in three portions at 20 min intervals. The resulting green solution of $NaW_2Cl_7(THF)_5$ was stirred for 12 h and then cannulated into a glass bomb reactor containing Na(silox) (4.73 g, 19.8 mmol). After 2 h of stirring at 25 °C, the resulting brown solution was heated in an 85 °C bath for 12 h. The THF was removed *in vacuo* and the solids were triturated with 30 mL of hexanes. The solids were resuspended in 50 mL of hexanes, filtered through Celite, and crystallized from hexanes to give 4.45 g of brown crystals (69% yield). Anal. Calcd for $W_2Cl_2Si_4O_4C_{48}H_{108}$: C, 44.34; H, 8.37. Found: C, 44.21; H, 8.38.

2. $[(silox)_2WCH_3]_2$ (2). Into a flask containing **1** (520 mg, 0.400 mmol) in 5 mL of Et_2O was syringed CH_3MgBr (3.0 M in Et_2O, 0.4 mL, 1.2 mmol). After 6 h of stirring at 25 °C, the solvent was removed *in vacuo*, and the residue was filtered off in hexanes. The salt cake was repeatedly washed to remove all traces of green product; then the filtrate was concentrated to 3 mL, cooled to −78 °C, and filtered to yield dark green crystals of **2** (470 mg, 81% yield). Anal. Calcd for $W_2Si_4O_4C_{50}H_{114}$: C, 47.68; H, 8.85. Found: C, 46.29; H, 9.12.

3. $[(silox)_2WH]_2$ (3). a. Reduction of 1 under H_2. Into a flask containing **1** (735 mg, 0.565 mmol) and 0.9% Na/Hg (1.187 mmol Na) was distilled 5 mL of DME. H_2 (1 atm) was admitted and the solution warmed to 25 °C with stirring. After 15 min, the solvent and volatiles were removed *in vacuo*, the solid was triturated three times with hexanes, and the product was filtered off. The salt cake was washed with hexanes until no brown material remained. Crystallization from 2 mL of hexanes at −78 °C gave yellow-brown crystals of **3** (490 mg, 70% yield). IR (Nujol): 1995 cm^{-1}.

b. Hydrogenation of 2. A 50 mL bomb reactor was charged with 0.278 g (0.22 mmol) of **2** and 6 mL of toluene. Dihydrogen (750 Torr) was admitted, and the bomb was sealed and heated to 60 °C for 14 h. Removal of all gases and transfer of the solution to another flask permitted isolation of yellow-brown, microcyrstalline **3** upon removal of the solvent. The conversion to **3** occurred in >96% purity, according to ^{1}H NMR spectroscopy. Anal. Calcd for $W_2Si_4O_4C_{48}H_{110}$: C, 46.82; H, 9.00. Found: C, 46.89; H, 9.33.

4. $[(silox)_2WCH_2CH_3]_2$ (5). A flask containing **3** (223 mg, 0.181 mmol) in 3 mL of hexanes was exposed to 1 atm of ethylene, causing immediate darkening. After 1 h of stirring at 25 °C, the volatile materials were quickly removed *in vacuo*, and the resulting brown-black solid was collected without further purification and stored at −20 °C. NMR analysis revealed quantitative conversion to **5**, but loss of ethylene became evident, and total reversion to **3** occurred within hours. The thermal instability precluded elemental analysis.

5. $(silox)_2HW{\equiv}W(OSi^tBu_2CMe_2CH_2)(silox)$ (6). a. NMR tube scale thermolysis of 3. Into an NMR tube charged with **3** (20 mg, 0.016 mmol) and attached to a needle valve adapter was distilled 0.5 mL of C_6D_6. The tube was flame-sealed and thermolyzed at 100 °C for 4 h, resulting in the formation of 60% **6** by ^{1}H NMR analysis.

b. Extended Thermolysis of 3. In a 50 mL bomb reactor, 250 mg of **3** (0.20 mmol) was thermolyzed in 15 mL of cyclohexane at 70 °C for 5 d. During this period, evolved H_2 was removed via eight freeze−pump−thaw degas cycles. ^{1}H NMR spectroscopic analysis revealed ∼77% conversion to **6** after 2 d and complete (>98%) conversion to a 3:1 **6a**:**6b** ratio of rotational isomers after 5 d, but this became 1:1.5 upon extended thermolysis (15 d, 70 °C) in C_6D_6. Addtional resonances suggested that a third rotational isomer could be present (∼15%), but overlapping resonances prevented spectral comparison.

c. Reduction of 1. Into a flask containing **1** (600 mg, 0.461 mmol) and 0.9% Na/Hg amalgam (2.36 g, 0.923 mmol (Na)) at −78 °C was distilled 5 mL of DME. The brown solution was warmed to 25 °C and stirred. No color change was observed as salts formed (15 min). The solution was stirred for 2 h, and the solvent was removed. The residues were triturated three times with hexanes and then filtered off in hexanes. Reducing the volume of hexanes to 2 mL and cooling to −78 °C gave 140 mg of reddish brown **6** (25% yield). Anal. Calcd for $W_2Si_4O_4C_{48}H_{108}$: C, 46.90; H, 8.85. Found: C, 46.01; H, 8.83.

6. NMR Tube Scale Experiments. a. $(silox)_2MeW{\equiv}WH(silox)_2$ (4). Into an NMR tube charged with 25 mg of **2** (0.020 mmol) and attached to a needle valve adapter was distilled 0.5 mL of C_6D_6. Dihydrogen (29 Torr) was admitted to the tube at 77 K, and the tube was flame-sealed. After 20 min at 70 °C, ^{1}H NMR spectroscopy revealed the presence of **4** in the reaction mixture (∼20%). ^{1}H NMR: δ 3.96 (s, J_{WH} = 11.4 Hz, 3H, WMe), 19.51 (s, J_{WH} = 335 Hz, 1 H, WH).

b. $[(silox)_2WCl]_2(\mu\text{-}H)_2$ (8). An NMR tube was charged with a solution of **1** (15 mg, 0.12 mmol) in 0.6 mL of toluene-d_8 and attached to a needle valve adapter. The solution was freeze−pump−thaw degassed and cooled to 77 K. H_2 (700 Torr) was admitted, and the tube was flame-sealed.

Physical Studies. 1. Equilibrium of 3 + H_2 ⇌ $[(silox)_2W]_2(\mu\text{-}H)_4$ (7). An NMR tube charged with 20 mg (0.016 mmol) **3** in 0.7 mL of toluene-d_8 was attached to a needle valve adapter. The solution was freeze−pump−thaw degassed, 700 Torr of H_2 was admitted at 77 K, and the tube was flame-sealed. ^{1}H NMR spectra were recorded using a 20-s delay between pulses, and H_2 concentrations were measured

(57) (a) Schrock, R. R.; Sturgeoff, L. G.; Sharp, P. R. *Inorg. Chem.* **1983**, *22*, 2801−2806. (b) Cotton, F. A.; Felthouse, T. R. *Inorg. Chem.* **1981**, *20*, 3880−3886. (c) Canich, J. A. M.; Cotton, F. A. *Inorg. Chim. Acta* **1988**, *142*, 69−74.

(58) (a) Canich, J. M.; Cotton, F. A.; Daniels, L. M.; Lewis, D. B. *Inorg. Chem.* **1987**, *26*, 4046−4050. (b) Agaskar, P. A.; Cotton, F. A.; Dunbar, K. R.; Falvello, L. R.; O'Connor, C. J. *Inorg. Chem.* **1987**, *26*, 4051−4057. (c) Canich, J. M.; Cotton, F. A.; Dunbar, K. R.; Falvello, L. R. *Inorg. Chem.* **1988**, *27*, 804−811. (d) Partigianoni, C. M.; Nocera, D. G. *Inorg. Chem.* **1990**, *29*, 2033−2034.

(59) Santure, D. J.; Sattelberger, A. P. *Inorg. Synth.* **1989**, *26*, 219−225.

by comparing the integrated intensity of the H_2 signal versus those of the tungsten hydride signals. $^{29}Si\{^1H\}$ spectra were obtained using an initial solution of 50 mg of **3** in 0.7 mL of toluene-d_8, with 0.05 mL of $(Me_3Si)_2O$ added as an internal standard. The ^1H broad-band decoupler was centered on the silox resonance, and the pulse delay was set to 30 s. Direct measurements of integrated intensities of **3**, H_2, and **7** in the ^1H NMR spectrum were obtained over a 25.9−88.7 °C temperature range. Data (T (°C), K_{eq} (M^{-1})): 25.9, 246.2; 30.8, 210.6; 35.6, 169.3; 40.4, 127.4; 45.2, 111.0; 50.0, 76.3; 54.9, 63.5; 59.7, 49.8; 64.5, 46.6; 69.4, 37.7; 74.2, 26.5; 79.0, 26.0; 83.8, 18.4; 88.7, 14.2. A plot of ln K_{eq} vs $1/T$ yielded thermodynamic parameters: $\Delta H° = -9.6(4)$ kcal/mol, $\Delta S° = -21(2)$ eu (1 M standard state).

2. Evans' Method[43] Attempt To Observe Excited State. In a volumetric flask, **3** (42 mg, 81% purity) was dissolved in 1.0 mL of C_6D_6. The solution was transferred to a flame-dried NMR tube attached to a 14/20 joint. A sealed capillary tube containing C_6D_6 was added to the tube, which was then attached to a needle valve, brought to the vacuum line, cooled to 77 K, and evacuated. Dihydrogen (500 Torr) was admitted at 77 K to the headspace above the frozen solution, and the tube was sealed with a torch. The tube was heated to 90 °C in the NMR spectrometer probe, and a ^1H NMR spectrum revealed a 4.8:2.24:1 mixture of **6**:**3**:**7**; **7** comprised ∼12.4% of the bimetallic species present, and its concentration was ∼5.2 mg/mL. The line width of the C_6D_5H resonance was 5.46 Hz at 90 °C, and no other resonances were observed in the region. Assuming a $\Delta E = 745$ cm^{-1} for the singlet−triplet splitting, the triplet state should be 13.5% populated at 363 K, resulting in an effective concentration of paramagnetic material of ∼0.7 mg/mL (5.7×10^{-4} M), and would result in a paramagnetic line shift of the C_6D_5H reference of 0.9 Hz, which is not experimentally verifiable.

Calculations. Extended Hückel parameters used are as follows: W(6s), $H_{ii} = -8.26$, $\zeta_1 = 2.341$; W(6p), $H_{ii} = -5.17$, $\zeta_1 = 3.309$; W(5d), $H_{ii} = -10.37$, $\zeta_1 = 4.982$, $c_1 = 0.6685$, $\zeta_2 = 2.068$, $c_2 = 0.5424$; O(2s), $H_{ii} = -32.30$, $\zeta_1 = 2.275$; O(2p), $H_{ii} = -14.80$, $\zeta_1 = 2.275$; Si(3s), $H_{ii} = -17.30$, $\zeta_1 = 1.383$; Si(3p), $H_{ii} = -9.20$, $\zeta_1 = 1.383$; H(1s), $H_{ii} = -13.60$, $\zeta_1 = 1{,}300$.

Distances and angles used in the EHMO calculations can be found in the figure captions. W−O and O−Si distances were taken from the crystal structure determination of $[(silox)_2WCO]_2$.[37] The average $W-W-O_{silox}$ angle was 115°, and this value was used for calculations on $[(H_3SiO)_2W]_2$ (**9′**) but was changed to 120° for $[(H_3SiO)_2WH_2]_2$ (**7′**) due to unrealistic interactions between the $-OSiH_3$ ligands and the bridging hydrides. The interaction diagram for **9′** (Figure 4) was calculated using a typical W−W quadruple-bond distance,[32] while the FMOs for $(H_3SiO)_4W_2$ in Figure 5 were calculated at the geometry specified for the tetrahydride species, **7′**. Typical terminal and bridging W−H distances were chosen.[50]

Molecular mechanics calculations were performed using the CAChe Worksystem.[60] Geometries were optimized using the block-diagonal Newton−Raphson method.[61] Optimizations were performed to energy changes of less than 0.001 kcal/mol. Standard MM2 parameters[62] were used, with an augmented force field to handle the tungsten atoms. The effect of the augmented force field was minimized by locking in W−W and W−O distances, and the O−W−W−O dihedral angles.

Ab initio calculations were performed using GAMESS.[63] A valence-only basis with an extra p function on the hydrogens and d function on the oxygens was used with effective core potentials to describe the metal cores while the W 5s, 5p, 5d, and 6s electrons were treated explicitly.[53] Calculations were performed at the RHF/UHF level.

Acknowledgment. We gratefully acknowledge the National Science Foundation and Cornell University for support of this research. R.L.M. thanks the NSF and the Spencer T. and Ann W. Olin Foundation for fellowship support.

IC9513191

(60) CAChe Worksystem, Release 3.5, CAChe Scientific, 1993.
(61) For an overview of the Newton−Raphson method, see: Press, W. H.; Teukolsky, S.A.; Vetterling, W. T.; Flannery, B. P. *Numerical Recipes in FORTRAN*, 2nd ed.; Cambridge University Press: Cambridge, U.K., 1992; 372−375.
(62) Allinger, N. L. *J. Am. Chem. Soc.* **1977**, *99*, 8127−8134.
(63) Schmidt, M. W.; Baldridge, K. K.; Boatz, J. A.; Elbert, S. T.; Gordon, M. S.; Jensen, J. H.; Koseki, S.; Matsunaga, N.; Nguyen, K. A.; Su, S.; Windus, T. L.; Dupuis, M.; Montgomery, J. A. *J. Comput. Chem.* **1993**, *14*, 1347−1363.